Journal of Astrophysics & Aerospace Technology

Ali, J Astrophys Aerospace Technol 2018, 6:1
DOI: 10.4172/2329-6542.1000160

Review Article Open Access

# Shell Model for Study Quadrupole Transition Rates in B2 in Some Neon Isotopes in sd-shell with Using Different Interactions

**Ahmed H Ali***

*Department of Theoretical Nuclear Physics and Medical Physics, College of Medicine, University of Fallujah, Iraq*

**Abstract**

Quadrupole transition rates B(E2) and Bohr-Mottelson effective charges (B-M) were calculated for even-even 18,20,22,24,26,28Ne isotopes based on sd shell model space. One body transition matrix (OBTM) was calculated using the code NushellX@MSU with different interactions. Our calculation for the reduced transition probabilities B(E2) are compared with available experimental data.

**Keywords:** Quadrupole transition rates; Effective interaction; Shell model; Effective charges

## Introduction

Solving the nuclear many-body problem is a fundamental task in nuclear structure studies. The spherical shell model has continually been a reliable tool when comparing with experimental observables. In practical shell model calculations, the valence space is limited within one or several adjacent major shells. The bulk of its wave function is presumably contained in this restricted configuration space [1]. Nuclear shell model is one of the most powerful tools for giving a quantitative interpretation to the experimental data. The two main ingredients of any shell model calculations are the N-N interaction and the configuration space for valence particles. In principle one can either perform shell model calculations with realistic N-N interaction in unlimited configuration space or with renormalized effective interaction limited configuration space [2]. Shell model calculations are carried out within a model space in which the nucleons are restricted to occupy a few orbits. If appropriate effective operators are used taking into account the effect of the larger model space, the shell model provides a reasonable description of these observables [3]. The calculations of shell model, carried out within a model space in which the nucleons are restricted to occupy a few orbits are unable to reproduce the measured static moments or transition strengths without scaling factors. Calculations of transition strengths using the model space wave function alone are inadequate for reproducing the data. Therefore, effects out of the model space, which are called core polarization effects, are necessary to be included in the calculations [4]. A study of nuclei in the *sd* shell can thus lead to a better understanding between a microscopic description of the nucleus (shell model) and a macroscopic (collective) description [5]. The *sd*-shell nuclei are considered as an inert $^{16}$O core and the valence nucleons are distributed in $1d_{5/2}$, $2s_{1/2}$ and $1d_{3/2}$ shell. Higher configurations can be included through perturbation theory, where particle-hole excitations are allowed from the core and the valence nucleons to all allowed orbits with $n\hbar\omega$ excitations. The number $n$ depends on the convergence of the calculations. The deformation can be investigated experimentally and theoretically, through their electromagnetic transitions. The general trend of the $2^+$ excitation energy E ($2_1^+$) and the reduced electric quadrupole transition strength between the first excited $2^+$ state and the $0^+$ ground state, $B(E2, 0_1^+ \rightarrow 2_1^+$ for even-even nuclei are expected to be inversely proportional to one another [6]. States of mixed configurations the situation differs in the valence shell *sd* shell model for $N$ (neutron) > 8 and $p$ (proton) > 8). Figure 1 indicates how nucleons move via the nucleon–nucleon interaction. The occupancy pattern of nucleons over different orbits is called configuration [7].

## Theory

The theoretical calculations of the reduced quadrupole transition probability $B(E2; 0_1^+ \rightarrow 2_1^+)$ performed from calculated the reduced electric matrix element between the initial and final nuclear states is [8]:

$$\mathrm{M(EJ)} = \left\langle \mathrm{J_f} \left\| \sum_k \mathrm{e(k)\hat{o}_J(\vec{r})_k} \right\| \mathrm{J_i} \right\rangle \quad (1)$$

where $e(k)$ is the electric charge for the $k$-th nucleon. Since $e(k)$=0 for neutron, there should appear no direct contribution from neutrons; however, this point requires further attention: The addition of a valence neutron will induce polarization of the core into configurations outside the adopted model space. Such core polarization effect is included through perturbation theory which gives effective charges for the proton and neutron. The reduced electric matrix element can be written in terms of the proton and neutron contributions:

$$\mathrm{M}(EJ) = \sum_{t_z} e(t_z) \left\langle J_f \left\| \hat{o}_J(\vec{r}, t_z) \right\| J_i \right\rangle \quad (2)$$

where $\left\langle \mathrm{J_f} \left\| \hat{o}_J(\vec{r}, t_z) \right\| \mathrm{J_i} \right\rangle$ is the electric matrix element which is expressed as the sum of the products of the one-body transition matrix (*OBTM*) times the single-particle matrix elements,

$$\left\langle J_f \left\| \hat{o}_J(\vec{r}, t_z) \right\| J_i \right\rangle = \sum_{j\,j'} OBTM(J_i, J_f, J, t_z, j, j') \left\langle j' \left\| \hat{o}_J(\vec{r}, t_z) \right\| j \right\rangle \quad (3)$$

With $j$ and $j'$ label single-particle states for the shell model space.

The electric matrix element can be represented in terms of only the model space matrix elements by assigning effective charges ($e^{eff}$ ($t_z$)) to the neutrons and protons

$$M(EJ) = \sum_{t_z} e^{e\,f\,f}(t_z) \left\langle J_f \left\| \hat{o}_2(\vec{r}, t_z) \right\| J_i \right\rangle_{MS} \quad (4)$$

They formulated an expression for the effective charges to explicitly include neutron excess via [9]

$$e^{e\,f\,f}(t_z) = e(t_z) + e\delta e(t_z), \delta e(t_z) = Z / A - 0.32(N - Z) / A - 2t_z[0.32 - 0.3(N - Z) / A] \quad (5)$$

***Corresponding author:** Ahmed H. Ali, PhD in Theoretical Nuclear Physics and Medical Physics, College of Medicine, University of Fallujah, Iraq, Tel no: + 964-7815262642; E-mail: dr.ahmedphysics@uofallujah.edu.iq.

**Received** December 10, 2017; **Accepted** April 23, 2018; **Published** April 27, 2018

**Citation:** Ali AH (2018) Shell Model for Study Quadrupole Transition Rates in B2 in Some Neon Isotopes in sd-shell with Using Different Interactions. J Astrophys Aerospace Technol 6: 160. doi:10.4172/2329-6542.1000160

The reduced electric transition probability from $j_i$ to $j_f$ be defined as [8]:

$$B(EJ) = \frac{|M(EJ)|^2}{2J_i + 1} \quad (6)$$

## Results and Discussion

The calculation of the reduced electric transition probability $B(E2)$ from the ground $0^+$ state to the first excited $2^+$ state for some neon even-even $^{18,20,22,24,26,28}$Ne isotopes and which were performed by using equation (6). The one body transition matrix element (*OBTM*) values were obtained by the shell model calculations that performed via the computer code NuShellX [10] MSU and using different interactions such as *USDB* (Universal *sd*-shell interaction B) [11], USDA interaction (Universal *sd*-shell interaction A) [11] and Bonn-A interaction [12]. The reduced quadrupole transition probability is calculated using different effective charges such as conventional effective charges (*CEF*) [13], Bohr-Mottelson effective charges (B-M) [9,14] and standard effective charges (*ST*) $e_p$=1.36 and $e_n$=0.45 [14,15]. The radial wave functions for the single-particle matrix elements were calculated with the harmonic oscillator (HO) potential with size parameters for each isotope are calculated as

$0_1^+ \rightarrow 2_1^+$ with $\hbar\omega = 45A^{-1/3} - 25A^{-2/3}$ as shown in Table 1 [16].

The presented results for B(*E2*) values in this work were compared with the available experimental values give in reference [17].

### USDB Interaction

Reduced transition probabilities in units of $e^2fm^4$ are calculated for Neon Ne isotopes (Z=10) with mass number *A*=18, 20, 22, 24, 26, 28 and with neutron number *N*=8, 10, 12, 14, 16, 18, respectively. Shell model calculations in *sd* model space and USDB interaction [11] was used to generate the *OBTM* elements for the ground state with *J*=0 and excited state with *J*=2. The harmonic oscillator size parameter *b* [16] was calculated for each isotope and tabulated in Table 1. All isotopes in the present work composed of the core $^{16}$O nucleus plus two protons surrounding the core. These outer two protons are considered to move in the *sd* shell model space. The calculated reduced electric transition probability B($E$ 2; $0_1^+ \rightarrow 2_1^+$) using USDB interaction and different effective charges these results of the $B(E2)_{CEF}$, $B(E2)_{ST}$ and $B(E2)_{B\text{-}M}$ are displayed in Table 1 and plotted in Figure 2a as a function of neutron number *N* and mass number *A* in comparison with the experimental values [17]. The Bohr-Mottelson effective charges (B-M) [9] were calculated for $^{18,20,22,24,26,28}$Ne isotopes as shown in Table 1, Conventional effective charges (CEF) [13] which are for proton 1.3 *e* and for the neutron 0.5 *e* and standard effective charges (ST) [15] which are 1.36 *e* for the proton and 0.45 *e* for the neutron. The B(*E2*) were calculated for $^{18}$Ne where $B(E2)_{CEF}$=136, $B(E2)_{ST}$=149, and $B(E2)_{B\text{-}M}$=123, these values underestimates the measured data (experimental value) 243 ± 16 $e^2fm^4$ [17]. The B(*E2*) were calculated of $^{20}$Ne isotope where $B(E2)_{CEF}$=243.5 and $B(E2)_{ST}$=246.2, these values underestimate the experimental value 333 ± 16 $e^2fm^4$ except the calculated value of $B(E2)_{B\text{-}M}$=300.6 is very close to experimental value. The B(*E2*) were calculated of $^{22}$Ne isotope where $B(E2)_{CEF}$=246.6 and $B(E2)_{ST}$=244.8, these values agree well with the experimental value 229 ± 42 $e^2fm^4$ while the calculated value of $B(E2)_{B\text{-}M}$=279.1 is very close to experimental value. The B(*E2*) were calculated of $^{24}$Ne isotope where $B(E2)_{CEF}$=202, $B(E2)_{ST}$=202.6, these values close to experimental value $0_1^+ \rightarrow 2_1^+$ $e^2fm^4$ while the calculated value of $B(E2)_{B\text{-}M}$=191.4 agree with the experimental value. Also, B(*E2*) were calculated for $^{26}$Ne isotope where $B(E2)_{B\text{-}M}$ which agree with the experimental value 155 ± 32, while the calculated value of $B(E2)_{CEF}$ is close to the experimental value and the calculated value of $B(E2)_{ST}$ overestimate the experimental value. The B(*E2*) were calculated $^{28}$Ne isotope $B(E2)_{CEF}$ and $B(E2)_{B\text{-}M}$ values close to the experimental value 136 ± 32 while the calculated value of $B(E2)_{ST}$ agree with the experimental value. The excitation energies were calculated for $^{18,20,22,24,26,28}$Ne isotopes and are compare with the experimental values [17] and tabulated in Table 1 and plotted in Figure 2b which shows an inverse relation between the excitation energy and transition rate B(*E2*) [5]. Theoretical values overestimate the experimental values where the excitation energy for some isotopes were high when fill orbit such as *N*=14 and 16

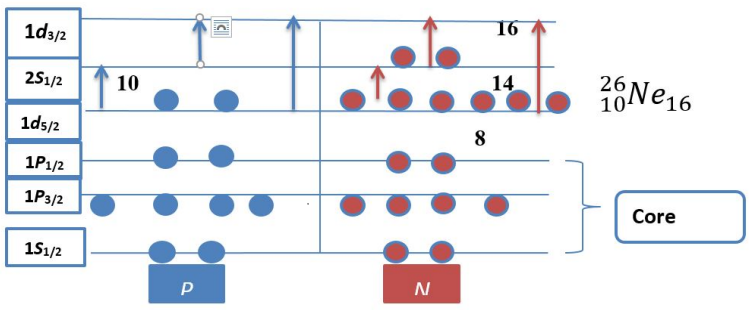


**Figure 1:** Distribution of nucleons (protons and neutrons) and their transfer to higher levels for the $^{26}$Ne isotope.

| $A_{10}$Ne | *b*(*fm*) | $(E_x)_{theo.}$(MeV) | $(E_x)_{exp.}$(MeV) | $B(E2)_{CEF}$ | $B(E2)_{ST}$ | $e_p$, $e_{n\ (B\text{-}M)}$ | $B(E2)_{B\text{-}M}$ | $B(E2)_{exp}$ |
|---|---|---|---|---|---|---|---|---|
| 18 | 1.750 | 1.99 | 1.887 | 136 | 149 | 1.24, 0.94 | 123 | 243 ± 16 |
| 20 | 1.773 | 1.746 | 1.663 | 243.5 | 246.2 | 1.18, 0.82 | 300.6 | 333 ± 16 |
| 22 | 1.794 | 1.363 | 1.274 | 246.6 | 244.8 | 1.13, 0.72 | 279.1 | 229.8 ± 42 |
| 24 | 1.814 | 2.111 | 1.981 | 202 | 202.6 | 1.09, 0.63 | 191.4 | 143+57-24 |
| 26 | 1.833 | 2.063 | 2.018 | 195.8 | 204 | 1.06, 0.56 | 147 | 155 ± 32 |
| 28 | 1.850 | 1.623 | 1.30 | 175 | 122.9 | 1.03, 0.50 | 180.2 | 136 ± 32 |

**Table 1:** The reduced electric transition probability B(E2) in units of $e^2$ $fm^4$ and excitation energies for Ne isotopes (*Z*=10). Experimental $E_x$ and *B*(*E2*) are taken from Reference [17]. Calculations B(E2) using USDB interaction [11] and set effective charges, conventional effective charges (*CEF*) *ep*=1.3 and *en*=0.5 [13], Bohr-Mottelson effective charges (*B-M*) [9], and standard effective charges (*ST*)*ep*=1.36 and *en*=0.45 [15].

or isotope has the magic property such as $N$=8 as shown in Figure 2b while it is decreasing when $N$=10, 12 and 18.

## USDA Interaction

Reduced transition probabilities in units of $e^2fm^4$ are calculated for Neon Ne isotopes (Z=10) with mass number $A$=18, 20, 22, 24, 26, 28 and with neutron number $N$=8, 10, 12, 14, 16, 18, respectively. Shell model calculations in *sd* model space and USDA interaction [11] was used to generate the *OBTM* elements for the ground state with $J$=0 and excited state with $J$=2. The harmonic oscillator size parameter [16] was calculated for each isotope and tabulated in Table 1. All isotopes in the present work composed of the core $^{16}$O nucleus plus two protons surrounding the core. These outer two protons are considered to move in the *sd* shell model space. The calculated reduced electric transition probability B($E$ 2; $0_1^+ \rightarrow 2_1^+$) using USDA interaction and different effective charges these results of the $B(E2)_{CEF}$, $B(E2)_{ST}$ and $B(E2)_{B\text{-}M}$ are displayed in Table 2 and plotted in Figure 3a as a function of neutron number $N$ and mass number $A$ in comparison with the experimental values [17]. The Bohr-Mottelson effective charges (B-M) [9] were calculated for $^{18,20,22,24,26,28}$Ne isotopes as shown in Table 2, Conventional effective charges (CEF) [13] which are for proton 1.3 $e$ and for the neutron 0.5 $e$ and standard effective charges (ST) [15] which are 1.36 $e$ for the proton and 0.45 $e$ for the neutron. The B($E2$) were calculated of $^{18}$Ne isotope where $B(E2)_{CEF}$=136, $B(E2)_{ST}$=149, and $B(E2)_{B\text{-}M}$=123, these values underestimate the experimental value 243 ± 16 $e^2fm^4$ [17]. The B($E2$) were calculated of $^{20}$Ne isotope where $B(E2)_{CEF}$=242 and $B(E2)_{ST}$=244.6, these values underestimate the experimental value 333 ± 16 $e^2fm^4$ except the calculated value of $B(E2)_{B\text{-}M}$=298.7 is close

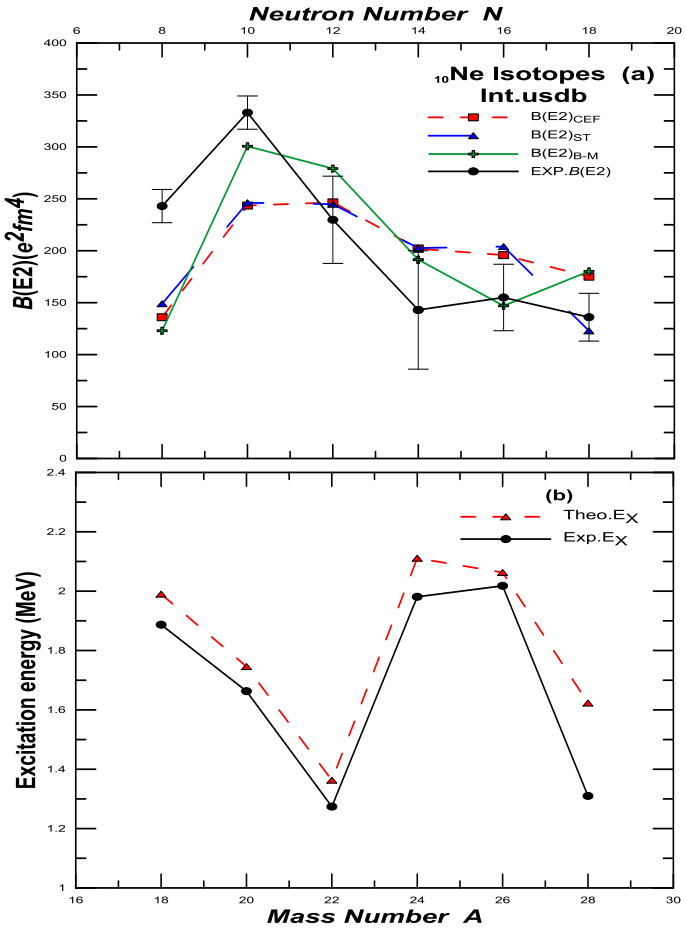


**Figure 2:** Calculated of B ($E2$; $0^+ \rightarrow 2^+$) and excitation energy of eve- even Ne isotopes. The experimental values are taken from Reference [17].

| $A_{10}$Ne | $b(fm)$ | $(E_x)_{theo.}$(MeV) | $(E_x)_{exp.}$(MeV) | $B(E2)_{CEF}$ | $B(E2)_{ST}$ | $e_p$ , $e_n$B-M | $B(E2)_{B\text{-}M}$ | B(E2)$_{exp}$ |
|---|---|---|---|---|---|---|---|---|
| 18 | 1.750 | 2.023 | 1.887 | 136 | 149 | 1.24, 0.94 | 123 | 243 ± 16 |
| 20 | 1.773 | 1.696 | 1.663 | 242 | 244.6 | 1.18, 0.82 | 298.7 | 333 ± 16 |
| 22 | 1.794 | 1.310 | 1.274 | 249.2 | 247.7 | 1.13, 0.72 | 280.4 | 229.8 ± 42 |
| 24 | 1.814 | 2.181 | 1.981 | 193 | 193.2 | 1.09, 0.63 | 184 | 143+57-24 |
| 26 | 1.833 | 2.086 | 2.018 | 195 | 203 | 1.06, 0.56 | 146 | 155 ± 32 |
| 28 | 1.850 | 1.645 | 1.30 | 175.8 | 181.4 | 1.03, 0.50 | 122.9 | 136 ± 32 |

**Table 2:** The reduced electric transition probability $B$(E2) in units of $e^2$ $fm^4$ and excitation energies for Ne isotopes ($Z$=10). Experimental $E_x$ and B($E2$) are taken from Reference [17]. Calculations B(E2) using USDA interaction [11] and set effective charges, conventional effective charges (*CEF*) *ep*=1.3 and *en*=0.5 [13], Bohr-Mottelson effective charges (*B-M*) [9], and standard effective charges (*ST*)*ep*=1.36 and *en*=0.45 [15].

to the experimental value. The B($E2$) were calculated of $^{22}$Ne isotope where B($E2$)$_{CEF}$=249.2 and B($E2$)$_{ST}$=247.7, these values agree with the experimental value 229 ± 42 $e^2fm^4$ while the calculated value of B($E2$)$_{B-M}$=280.4 is close to the experimental value. The B($E2$) were calculated of $^{24}$Ne isotope where B($E2$)$_{CEF}$=193, B($E2$)$_{ST}$=193.2 and B($E2$)$_{B-M}$=184, These values agree to the experimental value $143^{+57}_{-24}$ $e^2fm^4$. Also, B($E2$) were calculated for $^{26}$Ne isotope where B($E2$)$_{CEF}$ and B($E2$)$_{ST}$, these values overestimate the experimental value 155 ± 32 while the calculated value of B($E2$)$_{B-M}$ agrees very well with the experimental value. The B($E2$) were calculated for $^{28}$Ne isotope where B($E2$)$_{CEF}$ and B($E2$)$_{ST}$ values close to the experimental value 136 ± 32 while the calculated value of B($E2$)$_{B-M}$ agree with the experimental value. The excitation energies were calculated for $^{18,20,22,24,26,28}$Ne isotopes and are compare with experimental values and tabulated in Table 2 and plotted in Figure 3b which shows agreement theoretical values with experimental values except the excitation energies of $^{18,24,28}$Ne isotopes. For magic number $N$=8, the B($E2$) value is lower than those of $N \leq 18$, which corresponds to a maximum value of the excitation energy. The excitation energy is decreasing when $N$=12 to become minimum. The excitation energies will increase for $^{24,26}$Ne when $N$=14, 16 to become maximum because the neutrons in $^{24}$Ne fill the $0d_{5/2}$ orbit and in $^{26}$Ne fill the $1s_{1/2}$ orbit. The excitation energy is decrease when $N$=18 to become minimum because neutrons in $^{28}$Ne not fill $0d_{3/2}$ orbit. There are Similarities in the behavior of the excitation energies with USDB interaction and of the excitation energies with USDA interaction as shown in Figure 2b.

## SDBA interaction

Reduced transition probabilities in units of $e^2fm^4$ are calculated for Neon Ne isotopes (Z=10) with mass number $A$=18, 20, 22, 24, 26, 28 and with neutron number $N$=8, 10, 12, 14, 16, 18, respectively. Shell model calculations in *sd* model space and SDBA interaction [12] was used to generate the *OBTM* elements for the ground state with $J$=0 and excited state with $J$=2. The harmonic oscillator size parameter [16] was calculated for each isotope and tabulated in Table 1. All isotopes in the present work composed of the core $^{16}$O nucleus plus two protons surrounding the core. These outer two protons are considered to move in the *sd* shell model space. The calculated reduced electric transition probability B($E$ 2; $143^{+57}_{-24}$) using SDBA interaction and different effective charges these results of the B($E2$)$_{CEF}$, B($E2$)$_{ST}$ and B($E2$)$_{B-M}$ are displayed in Table 3 and plotted in Figure 4a as a function of neutron number $N$ and mass number $A$ in comparison with the experimental values [17]. The Bohr-Mottelson effective charges (B-M) [9] were calculated for $^{18,20,22,24,26,28}$Ne isotopes as shown in Table 3, Conventional effective charges (CEF) [13] which are for proton 1.3 $e$ and for the neutron 0.5 $e$ and standard effective charges (ST) [15] which are 1.36 $e$ for the proton and 0.45 $e$ for the neutron. The B($E2$) were calculated for $^{18}$Ne isotope where B($E2$)$_{CEF}$=137, B($E2$)$_{ST}$=147, and B($E2$)$_{B-M}$=122.4, these values underestimate the measured data (experimental value) 243 ± 16 $e^2fm^4$ [17]. The B($E2$) were calculated for $^{20}$Ne isotope where B($E2$)$_{CEF}$=247.5 and B($E2$)$_{ST}$=250, these values underestimate the experimental value 333 ± 16 $e^2fm^4$ except the calculated value of B($E2$)$_{B-M}$=305.5 is close to experimental value. The B($E2$) were calculated

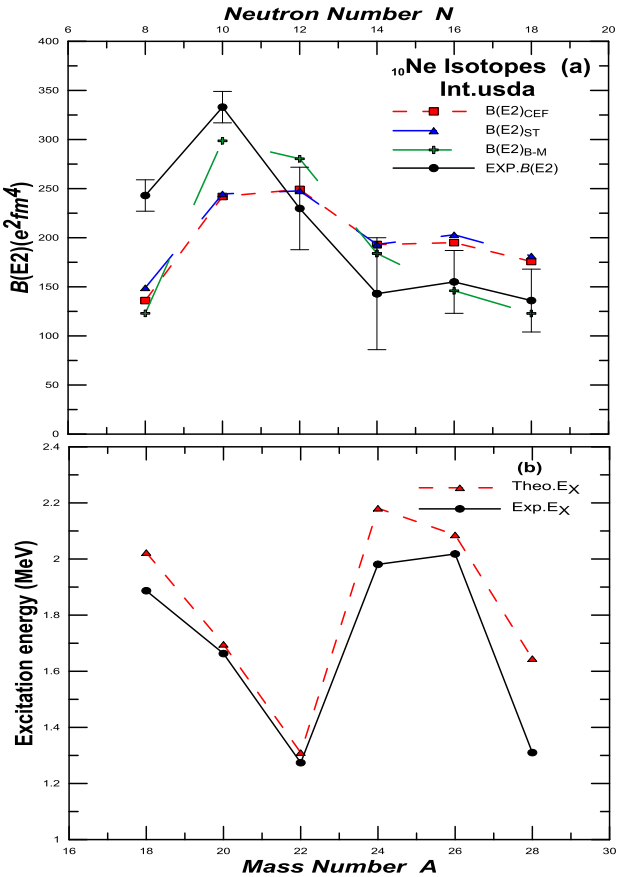


**Figure 3:** Calculated of B ($E2$; $0^+ \rightarrow 2^+$) and excitation energy of eve- even Ne isotopes. The experimental values are taken from Reference [17].

| $A_{10}Ne$ | $b(fm)$ | $(E_x)_{theo.}$(MeV) | $(E_x)_{exp.}$(MeV) | $B(E2)_{CEF}$ | $B(E2)_{ST}$ | $e_p$ , $e_n$ B-M | $B(E2)_{B-M}$ | $B(E2)_{exp}$ |
|---|---|---|---|---|---|---|---|---|
| 18 | 1.750 | 1.695 | 1.887 | 135 | 147 | 1.24, 0.94 | 122.4 | 243 ± 16 |
| 20 | 1.773 | 1.656 | 1.663 | 247.5 | 250 | 1.18, 0.82 | 305.5 | 333 ± 16 |
| 22 | 1.794 | 1.252 | 1.274 | 242 | 244 | 1.13, 0.72 | 280 | 229.8 ± 42 |
| 24 | 1.814 | 1.642 | 1.981 | 234 | 234.3 | 1.09, 0.63 | 242 | 143+57-24 |
| 26 | 1.833 | 1.708 | 2.018 | 240.4 | 244 | 1.06, 0.56 | 193 | 155 ± 32 |
| 28 | 1.850 | 1.648 | 1.30 | 210 | 217.5 | 1.03, 0.50 | 146.5 | 136 ± 32 |

**Table 3:** The reduced electric transition probability B(E2) in units of $e^2\,fm^4$ and excitation energies for Ne isotopes ($Z$=10). Experimental $E_x$ and $B(E2)$ are taken from Reference [17]. Calculations B(E2) using SDBA interaction [12] and set effective charges, conventional effective charges (*CEF*) *ep*=1.3 and *en*=0.5 [13], Bohr-Mottelson effective charges (*B-M*)[9], and standard effective charges (*ST*) *ep*=1.36 and *en*=0.45 [15].

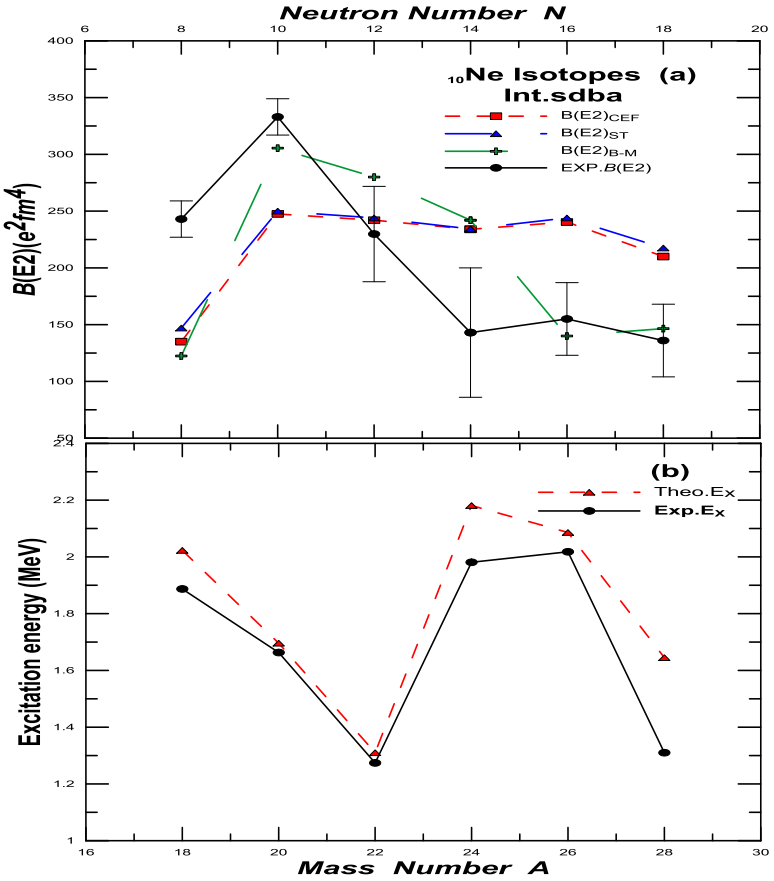


**Figure 4:** Calculated of B ($E2$; $0^+ \rightarrow 2^+$) and excitation energy of eve- even Ne isotopes. The experimental values are taken from reference [17].

for $^{22}$Ne isotope where $B(E2)_{CEF}$=242 and $B(E2)_{ST}$=244, these values agree with the experimental value 229 ± 42 $e^2fm^4$ while the calculated value of $B(E2)_{B-M}$=280 is close to experimental value. The B($E2$) were calculated for $^{24}$Ne isotope $B(E2)_{CEF}$=234, $B(E2)_{ST}$=234.3 and $B(E2)_{B-M}$=242, these values overestimate the experimental value $^{143}_{-24}$ $e^2fm^4$. Also, B($E2$) were calculated for $^{26}$Ne isotope where $B(E2)_{CEF}$ and $B(E2)_{ST}$, these values overestimate the experimental value 155 ± 32 while the calculated value of $B(E2)_{B-M}$, is close to the experimental value. The B($E2$) were calculated for $^{28}$Ne isotope where $B(E2)_{CEF}$ and $B(E2)_{ST}$, these values overestimate the experimental value 136 ± 32 while the calculated value of $B(E2)_{B-M}$ agree with the experimental value. The excitation energies were calculated for $^{18,20,22,24,26,28}$Ne isotopes and are compare with experimental values and tabulated in Table 3 and plotted in plotted in Figure 4b which shows the theoretical values agree to the experimental values, except the excitation energies of $^{18,24,28}$Ne isotopes. For magic number $N$=8, the B($E2$) value is lower, which corresponds to a maximum value of the excitation energy. The excitation energy is decreasing when $N$=12 to become minimum and the excitation energy will increase when $N$=14, 16 because the neutrons in $^{24,26}$Ne isotopes fill the $0d_{5/2}$ orbit and the $1s_{1/2}$ orbit, respectively. The excitation energy is decrease when $N$=18 because the neutrons not filled the $d_{3/2}$ orbit as shown in Figure 4b [18].

## Conclusion

Shell model was adopted to calculate transition rates B($E2$) of even-even Ne (18, 20, 22, 24, 26, and 28) isotopes including core-polarization effects through taken effective charges. Calculations B($E2$) with USDB interaction are better when using Bohr-Mottelson effective charges (B-M). Our results showed a decrease in the transition rates B($E2$) from the experimental value at the magic number $N$=8 while increasing

the excitation energy. Calculations excitation energy for even-even Ne isotopes which adopted on USDA interaction is best from other interactions in the present work. Excitation energy increasing for isotope which has magic number also when neutrons are fill orbit. Excitation energy is inversely proportional to transition rates B(*E2*). In SDBA interaction, results of the B(*E2*) are approximatly similar when using standard effective charges or conventional effective charges. Results of the B(*E2*) by using USDA interaction with B-M effective charges are better.

## References

1. Hailiang MA, Baoguo D, Yuliang Y (2012) Microscopic effective charges and the *B*(*E*2) values of terminating states in mirror nuclei $^{51}$Mn and $^{51}$Fe. Plasma Science and Technology 14: 603.
2. Srivastava PC, Mehrotra I (2009) Large scale shell model calculations for even-even $^{62-66}$Fe isotopes. Nuclear Theory 36.
3. Brown BA, Arima A, McGrory JB (1977) E2 core-polarization charge for nuclei near $^{16}$O and $^{40}$Ca. Nuclear Physics 277.
4. Radhi RA, Flaiyh GN, Raheem EM (2015) Electric quadrupole transitions of some even-even isotopes. Iraqi Journal of Science 56: 1047-1060.
5. Akiyama Y, Arima A, Sebe T (1969) The structure of the SD shell nuclei: (IV).$^{20}$Ne, $^{21}$Ne, $^{22}$Ne, $^{22}$Na and $^{24}$Mg. Nuclear Physics 138: 273-304.
6. Raman S, Nestor CW, Tikkanen P (2001) Transition probability from the ground to the first-excited 2+ state of even–even nuclides. Atomic Data and Nuclear Data Table 78: 1-128.
7. Otsuka T (2009) Shell structure of exotic nuclei. Lecture notes in Physics 3: 1-25.
8. Brussaard PJ, Glademans PWM (1977) Shell-model application in nuclear spectroscopy. North-Holland Publishing Company. Amsterdam.
9. De Forest T, Walecka JD (1966) Electron scattering and nuclear structure. Advances in Physics 15: 1-109.
10. Bohr A, Mottelson BR (1975) Nuclear Structure. Benjamin, New York, USA.
11. Brown BA, Rae WDM (2014) The shell-model code NuShellX@MSU. Nuclear Data Sheet.
12. Brown BA, Richter WA (2006) New USD Hamiltonians for the SD shell. Physical Review C 74: 034315.
13. Jensen MH, Kuo TTS, Osnes E (1995) Realistic effective interactions for nuclear systems. Physics Reports 261: 125-270.
14. Brown BA (2001) The nuclear shell model towards the drip lines. Progress in Particle and Nuclear Physics 47: 517-599.
15. Radhi RA, Alzubadi AA, Ali AH (2017) Calculations of the quadrupole moments for some nitrogen isotopes in P and PSD shell model spaces using different effective charges. Iraqi Journal of Science 58: 878-883.
16. Richter WA, Mkhize S, Brown BA (2008) SD-shell observables for the USDA and USDB Hamiltonians. Physical Review C 78: 064302.
17. Brown BA, Radhi R, Wildenthal BH (1983). Electric quadrupole and hexadecupole nuclear excitations from the perspectives of electron scattering and modern shell-model theory. Physics Reports 101: 313-358.
18. Pritychenko B, Birch M, Singh B, Horoi M (2016) Tables of E2 transition probabilities from the first 2+ states in even–even nuclei. Atomic Data and Nuclear Data Tables 107: 1-139.